J|A|C|S
ARTICLES
Published on Web 01/23/2008

Infrared Spectra of the $WH_4(H_2)_4$ Complex in Solid Hydrogen

Xuefeng Wang,[†] Lester Andrews,*[,†] Ivan Infante,[‡] and Laura Gagliardi[‡]

Department of Chemistry, University of Virginia, Charlottesville, Virginia 22904-4319, and Department of Physical Chemistry, University of Geneva, 30 Quai Ernest Ansermet, CH-1211 Geneva, Switzerland

Received September 21, 2007; E-mail: lsa@virginia.edu

Abstract: The codeposition of laser-ablated tungsten atoms with neat hydrogen at 4 K forms a single major product with a broad 2500 cm^{-1} and sharp 1860, 1830, 1782, 1008, 551, and 437 cm^{-1} absorptions, which are assigned to the $WH_4(H_2)_4$ complex on the basis of isotopic shifts and agreement with isotopic frequencies calculated by density functional theory. This D_{2d} structured complex was computed earlier to form exothermically from W atoms and hydrogen molecules. Annealing the matrix allows hydrogen to evaporate and the complex to aggregate and ultimately to decompose. Comparison of the H−H stretching mode at 2500 cm^{-1} and the W−H_2 stretching mode at 1782 cm^{-1} with 2690 and 1570 cm^{-1} values for the Kubas complex $W(CO)_3(PR_3)_2(H_2)$ suggests that the present physically stable $WH_4(H_2)_4$ complex has more strongly bound dihydrogen ligands. Our CASPT2 calculations suggest a 15 kcal/mol average binding energy per dihydrogen molecule in the $WH_4(H_2)_4$ complex.

Introduction

The coordination of dihydrogen to metals has attracted considerable attention since the Kubas tungsten complexes were first discovered.[1,2] A similar complex was later shown to undergo interconversion between the dihydrogen and dihydride subunits at room temperature in solution.[3] The first naked metal complex, $Pd(H_2)$, was prepared by Ozin and Garcia-Prieto in solid krypton and later investigated in solid argon and neon and also using density functional theory by Andrews et al.[4] The drive to form larger complexes with more dihydrogen has been motivated by the importance of hydrogen storage for potential use as a fuel.[5] In this regard calculations performed to search for stable larger complexes predicted that the stable $WH_4(H_2)_4$ complex (Figure 1) would form exothermically from tungsten atoms and six dihydrogen molecules.[6]

The first experimental investigation of naked W atoms reacting with dihydrogen performed in this laboratory found evidence for WH_4 as a major reaction product, and annealing the solid neon matrix increased a group of six sharp new absorptions, which were assigned to WH_6, as formed by the spontaneous reaction of WH_4 and H_2.[7] These absorptions matched density functional calculated frequencies for the distorted C_{3v} prism WH_6 structure, which remains the highest neutral hydride and the only neutral metal hexahydride to be observed experimentally. This distorted structure is more stable than the octahedral form, which has been the subject of extensive theoretical calculations from several groups.[8−11] It is significant that annealing the solid neon matrix into the 8−11 K range allows spontaneous reaction to increase the yield of both WH_4 and WH_6, but >220 nm irradiation increases nearby lower absorptions, and this cycle was found to be reversible.[7] One of

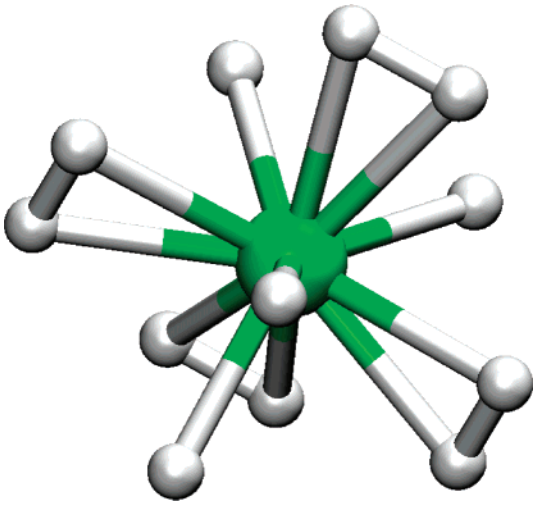

Figure 1. Structure of $WH_4(H_2)_4$ computed at the DFT level of theory.

[†] University of Virginia.
[‡] University of Geneva.

(1) (a) Kubas, G. J.; Ryan, R. R.; Swanson, B. I.; Vergamini, P. J.; Wasserman, H. J. *J. Am. Chem. Soc.* **1984**, *106*, 451. (b) Kubas, G. J.; Ryan, R. P.; Wrobleski, D. A. *J. Am. Chem. Soc.* **1986**, *108*, 1339. (c) Bender, B. R.; Kubas, G. J.; Jones, L. H.; Swanson, B. I.; Eckert, J.; Capps, K. B.; Hoff, C. D. *J. Am. Chem. Soc.* **1997**, *119*, 9179.
(2) (a) Kubas, G. J. Metal Dihydrogen and Sigma-bond Complexes. In *Modern Inorganic Chemistry*; Fackler, J. P., Jr., Ed.; Kluwer Academic/Plenum Publishers: New York, 2001, and references therein. (b) Crabtree, R. H. *Angew. Chem., Int. Ed. Engl.* **1993**, *32*, 789 and references therein.
(3) Khalsa, G. R. K.; Kubas, G. J.; Unkefer, C. J.; Van Der Sluys, L. S.; Kubat-Martin, K. A. *J. Am. Chem. Soc.* **1990**, *112*, 3855.
(4) (a) Ozin, G. A.; Garcia-Prieto, J. *J. Am. Chem. Soc.* **1986**, *108*, 3099. (b) Andrews, L.; Wang, X.; Alikhani, M. E.; Manceron, L. *J. Phys. Chem. A* **2001**, *105*, 3052 (Pd + H_2).
(5) Grochala, W.; Edwards, P. P. *Chem. Rev.* **2004**, *104*, 1283.
(6) Gagliardi, L.; Pyykko, P. *J. Am. Chem. Soc.* **2004**, *126*, 15015.
(7) Wang, X.; Andrews, L. *J. Am. Chem. Soc.* **2002**, *124*, 5636.
(8) Shen, M.; Schaefer, H. F., III.; Partridge, H. *J. Chem. Phys.* **1993**, *98*, 508.
(9) Kang, S. K.; Tang, H.; Albright, T. A. *J. Am. Chem. Soc.* **1993**, *115*, 1971.
(10) Kaupp, M. *J. Am. Chem. Soc.* **1996**, *118*, 3018.
(11) Tanpipat, N.; Baker, J. *J. Phys. Chem.* **1996**, *100*, 19818.

10.1021/ja077322o CCC: $40.75

these absorptions was described as perturbed [WH_4] and shown to be an intermediate for the production of WH_6 in a subsequent full paper.[12] We report here the reaction of laser ablated W atoms with neat normal and para-hydrogen and identify the largest possible physically stable tungsten hydride species, which is the tungsten tetrahydride tetradihydrogen complex calculated earlier.[6] Further quantum chemical calculations have been performed in order to assign the measured frequencies and to compare the stability of the various WH_n species possibly formed in the matrix isolation experiments.

Experimental and Computational Methods

The experiment for reactions of laser-ablated tungsten atoms with hydrogen molecules during condensation at 4 K has been described in detail previously.[13] The Nd:YAG laser fundamental (1064 nm, 10 Hz repetition rate with 10 ns pulse width) was focused onto a rotating tungsten target (Johnson-Matthey, 99.95%). The laser energy was varied from 5 to 20 mJ/pulse. Laser-ablated tungsten atoms were codeposited with 3−4 mmol of normal or para hydrogen[14] molecules onto a 4 K CsI cryogenic window for 30 min using a Sumitomo Heavy Industries Model RDK-205D cryocooler. Hydrogen (Matheson), D_2 and HD (Cambridge Isotopic Laboratories), and $H_2 + D_2$ mixtures were used in different experiments. FTIR spectra were recorded at 0.5 cm^{-1} resolution on a Nicolet 750 with 0.1 cm^{-1} accuracy using a HgCdTe range B detector. Matrix samples were annealed at different temperatures, and selected samples were subjected to broadband photolysis by a medium-pressure mercury arc lamp (Philips, 175 W) with the outer globe removed.

Quantum chemical calculations were performed using density functional theory (DFT), Moeller−Plesset perturbation theory (MP2), and multiconfigurational methods followed by second-order perturbation theory (CASSCF/CASPT2). The TURBOMOLE package[15] was employed for the DFT and MP2 calculations. Scalar relativistic effects were incorporated by employing on the tungsten atom the (8s7p6d2f1g)/[6s4p3d2f1g] effective core potential (ECP) basis set with 60 core electrons.[16] A valence triple-ζ basis set plus polarization functions, (5s2p1d)/[3s2p1d], was used on the hydrogen atoms. We will refer to this series of basis sets as TZVPP. The gradient-corrected BP86 exchange correlation functional was employed.[17,18] Full geometry optimization and frequency calculations were performed for all species at the DFT/BP86 level of theory. Some calculations were also repeated with the PBE functional.[19] The same ECP basis set was used for the MP2 calculations, in which all available electrons were correlated in the full virtual space.

The MOLCAS 7.0 package was employed for the CASSCF/CASPT2 calculations.[20] For CASSCF calculations on the WH_4 molecule, the orbitals formed by linear combinations of 6s as well as 5d orbitals on tungsten with 1s orbitals on the hydrogens were included in the active space, resulting in an active space formed of 10 electrons in 10 orbitals. The same active space was also employed in the calculations on $WH_4(H_2)_4$. For this species, calculations with 12 electrons in 12 orbitals and 14 electrons in 14 orbitals were also performed, in which these extra orbitals are delocalized on the H_2 moieties. In the subsequent CASPT2 calculations, no orbitals were frozen. This method has proven to be successful in the study of metal compounds.[21]

Coupled cluster calculations, with single and double excitations and perturbative triple excitations, CCSD(T), were also performed using the MOLCAS 7.0 package.[20] The same active space as that in the CASSCF calculations was employed. In total, 20 electrons were correlated for WH_4, and 38 electrons, for $WH_4(H_2)_4$. For both the CASSCF/CASPT2 and CCSD/CCSD(T) calculations the Douglas−Kroll−Hess approximation was employed to account for scalar relativistic effects.[22] All-electron basis sets of atomic natural orbital type, developed for relativistic calculations (ANO-RCC) with the Douglas−Kroll−Hess Hamiltonian, were used for all the atoms.[23] The contraction was 9s8p6d4f3g for W and 3s2p1d for H.

Results

Matrix-isolation infrared spectra are presented for laser ablated tungsten atom reactions with pure hydrogen samples. Density functional theoretical calculations of the structures and vibrational frequencies of tungsten hydrides and hydrogen complexes are given for comparison.

Infrared Spectra. Figure 2 illustrates infrared spectra in selected regions for tungsten ablation and reaction with pure normal hydrogen during condensation at 4 K. The most prominent new absorptions are observed at 1859.1, 1830.3, and 437.2 cm^{-1} with weaker bands at 2500, 1781.6, 1007.6, and 551.5 cm^{-1} (marked with arrows). The weak 1911.5 cm^{-1} feature is most likely due to WH_4 molecules on the surface as it falls below the strong 1920.5 cm^{-1} neon matrix counterpart for this molecule, which is the expected matrix shift relationship.[12,13] Annealing this sample to 6 K had little effect on the spectrum, while full arc irradiation (>220 nm) reduced the absorptions and a subsequent annealing to 6.3 K only sharpened them. The seven absorptions marked with arrows track together on annealing and UV irradiation, and they are thus associated with a common new product species. A final annealing to 7 K allowed the hydrogen matrix to evaporate and the new product to aggregate leaving behind no infrared absorptions (Figure 2b−e). The weak 1728.2 cm^{-1} band grows more on annealing and appears to be due to an aggregate species. Note the absence of absorptions in the 1920−2020 cm^{-1} region where the strongest absorptions of WH_6 appeared in solid neon.[7,12]

Two investigations with 99.9% para-hydrogen samples gave almost the same stronger absorptions, but since we can collect less para-hydrogen sample, the weaker bands were not observed. New slightly sharper bands were observed at 1912.6, 1859.7, 1830.9, 1782.0, 1732.8, 1000.8, and 436.5 cm^{-1}. Subsequent annealing and UV irradiation alternately sharpened and broadened these absorptions. The para-hydrogen environment produces sharper spectra for trapped species owing to the uniformity of $J = 0$ rotational state host molecules.[14,24]

In solid deuterium the weak WD_4 band[12] was observed at 1378.2 cm^{-1} along with a broad 1790 cm^{-1} band and new sharp absorptions at 1332.6, 1321.2, 1282.5, and 719.9 cm^{-1}. Irradiation (240−380 nm) increased these bands by 50%, but a full arc (>220 nm) reduced them slightly, as is illustrated in Figure

(12) Wang, X.; Andrews, L. *J. Phys. Chem. A* **2002**, *106*, 6720 (W + H_2).
(13) Andrews, L. *Chem. Soc. Rev.* **2004**, *33*, 123.
(14) (a) Silvera, I. F. *Rev. Mod. Phys.* **1980**, *52*, 393. (b) Andrews, L.; Wang, X. *Rev. Sci. Instrum.* **2004**, *75*, 3039.
(15) (a) Weigend, F.; Häser, M. *Theor. Chem. Acc.* **1997**, *97*, 331. (b) Weigend, F.; Häser, M.; Patzelt, H.; Ahlrichs, R. *Chem. Phys. Lett.* **1998**, *294*, 143. (c) Haase, H.; Ahlrichs, R. *J. Comput. Chem.* **1993**, *14*, 907. (d) Weigend, F.; Köhn, A.; Hättig, C. *J. Chem. Phys.* **2001**, *116*, 3175.
(16) (a) Andrae, D.; Haeussermann, U.; Dolg, M.; Stoll, H.; Preuss, H. *Theor. Chim. Acta* **1990**, *77*, 123. (b) Martin, J. M. L.; Sundermann, A. *J. Chem. Phys.* **2001**, *114*, 3408.
(17) Becke, A. D. *Phys. Rev. A* **1988**, *38*, 3098.
(18) Perdew, J. P. *Phys. Rev. B* **1986**, *33*, 8822.
(19) Perdew, J. P.; Burke, K.; Ernzerhof, M. *Phys. Rev. Lett.* **1996**, *77*, 3865.
(20) Karlstrom, G.; Lindh, R.; Malmqvist, P. A.; Roos, B. O.; Ryde, U.; Veryazov, V.; Widmark, P. O.; Cossi, M.; Schimmelpfennig, B.; Neogrady, P.; Seijo, L. *Comput. Mater. Sci.* **2003**, *28*, 222.
(21) Gagliardi, L. *Theor. Chem. Acc.* **2006**, *116*, 307.
(22) (a) Douglas, N.; Kroll, N. M. *Ann. Phys.* **1974**, *82*, 89. (b) Hess, B. *Phys. Rev. A* **1986**, *33*, 3742.
(23) Roos, B. O.; Lindh, R.; Malmqvist, P.-Å.; Veryazov, V.; Widmark, P. O. *J. Phys. Chem. A* **2005**, *108*, 2851.
(24) Momose, T.: Shida, T. *Bull. Chem. Soc. Jpn.* **1998**, *71*, 1 and references therein.

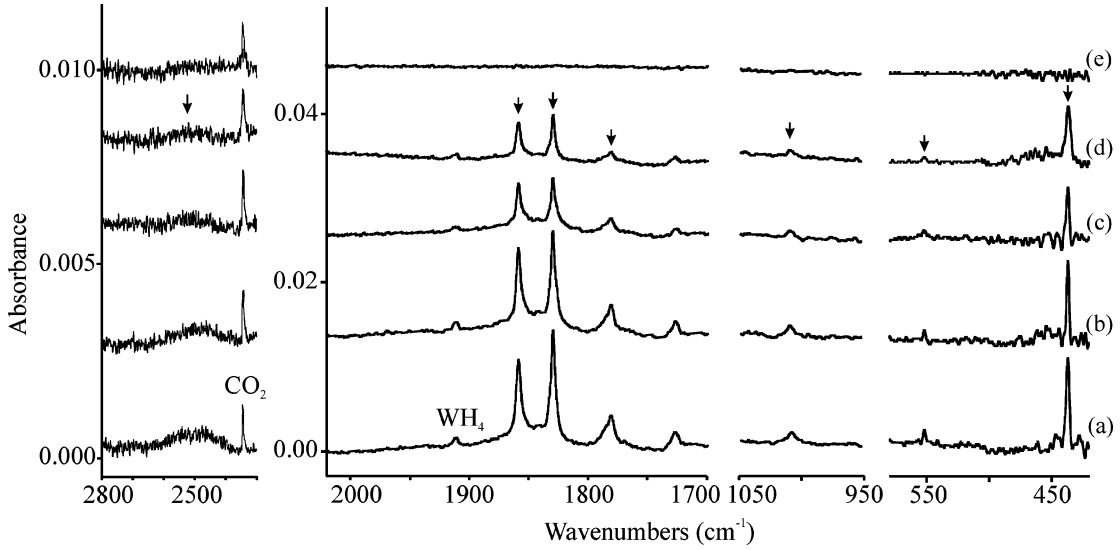

Figure 2. Infrared spectra for the laser-ablated W atom and pure hydrogen reaction product in solid normal hydrogen at 4 K. (a) Spectrum after reagent codeposition for 30 min, (b) after annealing to 6 K, (c) after >220 nm irradiation, (d) after annealing to 6.3 K, and (e) after warming to 7 K.

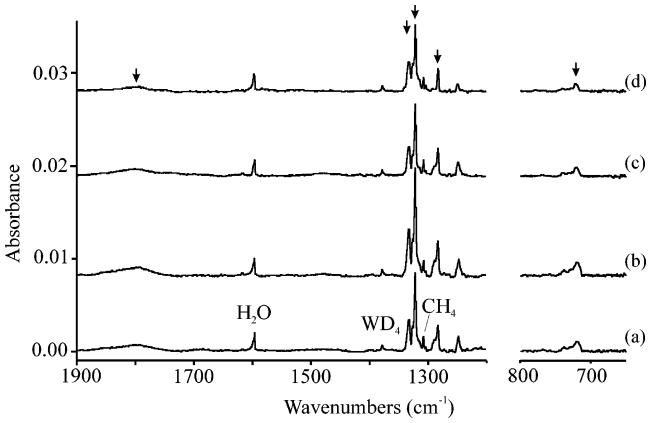

Figure 3. Infrared spectra for the laser-ablated W atom and normal deuterium reaction product trapped in the solid deuterium reagent at 4 K. (a) W + D_2, (b) after 240−380 nm irradiation, (c) after >220 nm irradiation, and (d) after annealing to 7.3 K. Arrows again denote new product absorptions.

3. The ortho-deuterium $J = 0$ rotational state host[14] produced slightly sharper bands shifted a few cm^{-1} (Table 1).

Mixed isotopic solid molecular hydrogen spectra are compared in Figure 4, and the absorptions are collected in Table 1. Absorptions in pure HD and H_2/D_2 are slightly shifted as these are different solid environments. No bands were observed in the 2200 or 1500 cm^{-1} regions with HD. A fringe structure prevented the observation of weak broad higher frequency bands with H_2/D_2.

Calculations

Since $WH_4(H_2)_4$ is the cluster most likely to be present in the matrix, we have focused our analysis on the aggregation of WH_4 with $4H_2$ molecules. The structures of the WH_4 and $WH_4(H_2)_4$ species have been optimized at the DFT and MP2 levels of theory. The relevant bond distances are reported in Table 2, and the harmonic vibrational frequencies are reported in Table 3. Other WH_n species and isotopic modifications have also been investigated, and their optimized structures and vibrational frequencies are reported in Supporting Information.

The agreement between seven measured and calculated frequencies identifies the $WH_4(H_2)_4$ species prepared in the matrix. In Table 3 we do not report BPE frequencies because they are very similar to the BP86 ones (they differ at most by a few wavenumbers). The DFT frequencies are closer to the measured frequencies than the MP2 values. It is well-known that wave function based methods, like MP2, suffer from basis-set incompleteness more than the DFT method. An estimate of the basis-set superposition error, using as dissociating fragments WH_4 and $4H_2$, shows an energy correction of 12 kcal/mol for the MP2 method, while it is less than 1 kcal/mol for DFT. As a consequence MP2 overestimates the bond strength between W and the H_2 moieties and predicts frequencies about 10−15% larger than DFT, in particular for the W−H(H_2) stretching modes. Despite this discrepancy, the seven fundamental peaks needed to describe the $WH_4(H_2)_4$ complex are also identified at the MP2 level.

CASSCF/CASPT2 single-point energy calculations were performed on WH_4 and the $WH_4(H_2)_4$ complex in order to examine the electronic structure of these two species. Electron density plots are shown below.

Discussion

The new infrared spectrum in solid hydrogen will be assigned to the highest tungsten hydride based on isotopic shifts and comparison with frequencies computed by density functional theory (DFT). The important mechanism for the W and hydrogen reaction will be considered.

Identification of $WH_4(H_2)_4$. The infrared spectra shown in Figure 2 reveal diagnostic absorptions due to molecular subunits that identify this new tungsten hydride dihydrogen complex. First, the WH_4 molecule in tetrahedral symmetry has been characterized by the triply degenerate antisymmetric W−H stretching and bending modes at 1920.5 and 525.2 cm^{-1} in solid neon,[12] and the weak new band at 1911.5 cm^{-1} in the solid hydrogen experiment can be assigned to WH_4 trapped on the surface where limited coordination can occur. The strong new absorptions at 1859.1 and 1830.3 cm^{-1} are slightly lower but still appropriate for W−H stretching modes as the 1.3951 and 1.3853 isotopic H/D frequency ratios indicate, and the new 551.5 cm^{-1} band is likewise due to an analogous H−W−H bending mode. Hence, the new product contains two or more W−H

Table 1. Infrared Absorptions (cm^{-1}) Observed from W Atom Reactions with Hydrogen in Solid Neon and Hydrogen Isotopic Samples

H_2/Ne	para-H_2	H_2	HD	$H_2 + D_2$	D_2	ortho-D_2	identification
		2500			1790		$WH_4(H_2)_4$
1920.5	1912.6	1911.5			1378.2	1378.5	WH_4/WD_4
1860.5	1859.7	1859.1	1859.7/1338.7	1857.2/1325.1	1332.6	1334.7	$WH_4(H_2)_4$
1832.2	1830.9	1830.3	1838.5/1318.8	1839.1	1321.2	1323.2	$WH_4(H_2)_4$
1785.1	1782.0	1781.6	1781.7/1263.2	1777.7/1280	1282.5	1285.4	$WH_4(H_2)_4$
		1728.2	1718, 1263		1247.7		W_xH_y/W_xD_y
999.6	1000.8	1007.6			719.9		$WH_4(H_2)_4$
	549.6	551.5					$WH_4(H_2)_4$
434.8	436.5	437.2					$WH_4(H_2)_4$

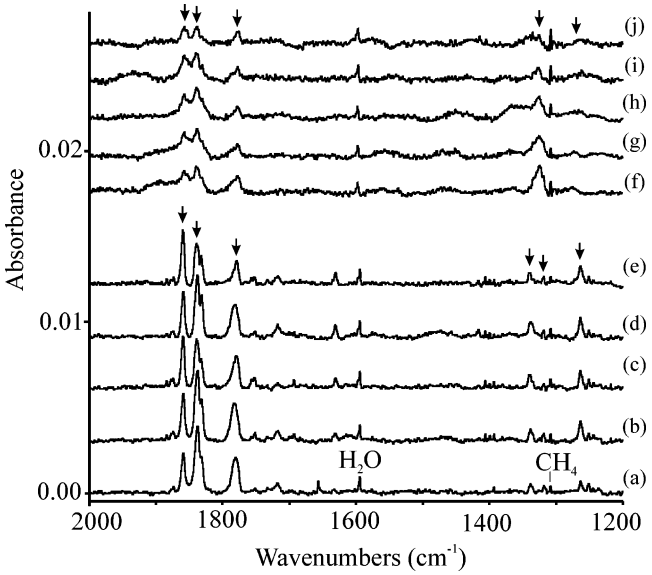

Figure 4. Infrared spectra for the laser-ablated W atom and mixed isotopic hydrogen reaction product trapped in the solid molecular hydrogen reagent at 4 K. (a) W + HD, (b) after 240−380 nm irradiation, (c) after annealing to 7 K, (d) after >220 nm irradiation, (e) after annealing to 7.5 K, (f) W + 50/50 $H_2 + D_2$ mixture, (g) after annealing to 6 K, (h) after annealing to 6.7 K, (i) after >220 nm irradiation, and (j) after annealing to 7.4 K.

Table 2. Bond Distances (Å) in $WH_4(H_2)_4$ at Various Levels of Theory[a]

	DFT/BP86	DFT/PBE	MP2
W−H	1.74 (1.71)	1.74(1.71)	1.72 (1.69)
W−H(H_2)	1.85	1.84	1.81
H−H(H_2)	0.88	0.89	0.87

[a] The TZVPP basis set has been employed in all DFT and MP2 calculations. The W−H bond length for WH_4 is given in parentheses for comparison.

hydride bonds. Second, the new absorptions at 2500, 1781.6, 1007.6, and 437.2 cm^{-1} arise from the presence of side-bound dihydrogen molecules in this new product. The broad 2500 cm^{-1} band is characteristic of the H−H stretching mode for strongly complexed dihydrogen molecules as this mode was first observed at 2690 cm^{-1} in the Kubas complex.[1a] The 2500/1790 = 1.397 H/D isotopic ratio is in accord with that expected for an H−H stretching mode. The 1781.6 cm^{-1} band can be assigned to the antisymmetric W−(H_2) stretching mode on the basis of its 1.3892 isotopic H/D frequency ratio and its prediction from density functional calculations to fall about 80 cm^{-1} below the aforementioned highest antisymmetric W−H stretching mode at 1859.1 cm^{-}. Such a mode was observed lower at 1570 cm^{-1} in the Kubas complex.[1a] The remaining two weak 1007.6 and strong 437.2 cm^{-1} bands are due to H_2−W−H_2 bending modes based on the prediction of such vibrational frequencies

Table 3. Frequencies (cm^{-1}) Calculated at the DFT/BP86/TZVPP Level of Theory for $WH_4(H_2)_4$ (Singlet State, D_{2d} Symmetry)

obs freq[a]	calc freq	int[b]	symm[c]	mode description
	351	0	b_1	
437.2	414	171	b_2	bending H_2−W−H_2
	428	6 × 2	e	bending H_2−W−H_2
	499	0	a_1	
	539	0	a_2	
551.5	565	38 × 2	e	bending H−W−H
	681	0	b_1	
	748	8 × 2	e	bending H−W−H_2
	775	0	a_2	
	816	16 × 2	e	bending H−W−H_2
	842	0	b_2	
	871	0	a_1	
	897	0	b_1	
1007.6	1065	172 × 2	e	bending H_2−W−H_2
	1160	3	b_2	bending H_2−W−H_2
	1284	0	a_1	
	1741	0	b_1	asym stretch W−H_2
	1767	0	a_2	stretch W−H_2
1782.0	1790	40 × 2	e	asym stretch W−H_2
1830.6	1844	212	b_2	sym stretch W−H
1859.3	1868	53 × 2	e	asym stretch W−H
	1903	0	a_1	totally sym stretch W−H
2500	2657	208 × 2	e	stretch H−H
	2683	11	b_2	stretch H−H
	2740	0	a_1	totally sym stretch H−H

[a] Observed here in solid hydrogen. [b]Calculated infrared intensity (km/mol). [c]Mode irreducible representation in D_{2d} symmetry.

at 1065 and 414 cm^{-1} by density functional theory (Table 3). The higher of these has the appropriate 1.3996 H/D isotopic frequency ratio, and the lower of these may be compared with the W−(H_2) deformation mode observed near 450 cm^{-1} for the Kubas complex.[1a]

This identification of $WH_4(H_2)_4$ based on the above vibrational assignments is confirmed by the comparison of the seven strongest observed and calculated frequencies in Table 3. First, a similar DFT calculation for WH_4 found a tetrahedral symmetry triplet ground state, in agreement with previous work,[12] and predicted the triply degenerate fundamentals at 1930 and 568 cm^{-1}, which are in very good agreement with the neon matrix 1920.5 and 525.2 cm^{-1} values that serve to calibrate the present calculations. The reaction product complex has symmetry reduced to D_{2d}, and the DFT prediction of e and b_2 W−H stretching modes at 1868 and 1844 cm^{-1} is in very good agreement with the strongest observed W−H stretching bands at 1859.1 and 1830.3 cm^{-1}. The antisymmetric degenerate (e) and antisymmetric combination of symmetric (b_2) H−W−H stretching modes is further confirmed by comparing harmonic calculated H/D ratios (1.4109, 1.4012) with the observed ratios (1.3951, 1.3853, respectively). The slightly lower H/D ratio is due to more W participation in the symmetric normal mode, which follows for the lower calculated and observed H/D ratios.

The observed H/D ratios are both lower than the harmonic calculated values owing to anharmonicity in the observed frequencies. Note from the experimental spectrum that the 1830.3 cm^{-1} band is 1.5 times stronger than the 1859.1 cm^{-1} absorption. Our calculation predicts the relative infrared intensities as 212/106, which is as accurate as can be expected for these calculations. Finally, the doubly degenerate H−W−H bending mode predicted at 565 cm^{-1} for $WH_4(H_2)_4$ is observed at 551.5 cm^{-1}: such an agreement is as good as can be expected for this mode and molecule.

The four modes involving the W−(H_2) linkage predicted at 2657, 1790, 1065, and 414 cm^{-1} are observed slightly lower except for the lowest frequency bending mode, which is observed slightly higher. The important diagnostic H−H stretching mode is observed as a broad band at 2500 cm^{-1}. [This is of course dominated by the strong calculated e mode, but the weaker b_2 mode is too close to be resolved for such a broad absorption (Table 3).]

Overall this agreement is excellent, and it confirms the present preparation of the $WH_4(H_2)_4$ tungsten hydride dihydrogen complex. Typically density functional theory overestimates observed frequencies owing in part to the lack of anharmonic correction,[25] and the overestimates are consistent for the strong W−H stretching modes calculated and observed here.

Finally, based on the ligand H−H stretching and W−H_2 stretching frequencies for the important Kubas complex $W(CO)_3(PR_3)_2(H_2)$, namely 2690 and 1570 cm^{-1}, and our most stable tungsten hydride dihydrogen complex, $WH_4(H_2)_4$, 2500 and 1782 cm^{-1}, the dihydrogen ligands are bound more strongly in $WH_4(H_2)_4$ than in the Kubas complex.[1a] This is consistent with the measured 7 kcal/mol H_2 binding enthalpy for the $W(CO)_3(PCy_3)_2(H_2)$ complex[1c] and our CASPT2 calculated average 15 kcal/mol binding energy for the$WH_4(H_2)_4$ complex (see below). Although $WH_4(H_2)_4$ cannot yet be prepared in synthetic quantities, it does represent the most stable hydride species that can be formed from W atoms and dihydrogen molecules, both computationally[6] and experimentally.

Neon Matrix Reactions. The W and H_2 reaction was first investigated in solid neon where the unique WH_6 molecule and the WH_4 precursor were identified from W−H stretching modes at 2021, 2004, 1954, and 1927 cm^{-1} and at 1920 cm^{-1}, repectively.[7,12] Other features at 1925.7 and 1911.5 cm^{-1} were recognized as an intermediate related through annealing and UV irradiation interconversion to WH_6. Since the $WH_4(H_2)$ complex is unstable in favor of WH_6 (the former converges to the latter on calculation), this intermediate was first suggested as $WH_2(H_2)_2$ and later as $(WH_4)(Ne)_x(H_2)$. In addition strong absorptions at 1860.2 and 1831.9 cm^{-1} in the initial solid neon deposit were assigned to WH and WH_2 on the basis of deuterium shifts, HD shifts, and clear-cut trends in the calculated W−H stretching frequencies.[12] Notice the 30% growth in the latter two bands (Figure 1, ref 7) on annealing to 10 K. At the time of this earlier work, we did not have a sample window cold enough to deposit solid hydrogen, namely 4 K, so the spectrum in Figure 2 was not available to contribute to our interpretation of W and H_2 reaction products. The neon matrix experiment was repeated with 6% H_2, and the product absorptions were stronger at 1860.5, 1832.2, and 1785.1 cm^{-1} along with weaker bands at 999.6 and 434.8 cm^{-1}. A fringe structure prevented the measurement of a band in the 2500 cm^{-1} region. Notice now the agreement between the former two neon matrix bands at 1860.2 and 1831.9 cm^{-1} and the present hydrogen matrix bands at 1859.1 and 1830.3 cm^{-1} both in profile and band position and recognize the small red shift expected from solid neon to solid hydrogen.[13] In addition the lower three bands measured in solid neon involving the W−(H_2) linkage are in good agreement with the solid hydrogen values. It is clear that the H_2 reagent is mobile enough upon condensation in excess neon at 4 K to effect sufficient aggregation to attain the most stable product that is also formed in pure solid hydrogen. Under these conditions WH and WH_2 are probably too reactive to survive and be trapped. Hence, the latter neon matrix bands must be reassigned to the $WH_4(H_2)_4$ tungsten hydride dihydrogen complex in solid neon.

This means that intervening bands must be considered for intermediate species such as $WH_6(H_2)_{1,2}$. In this regard new calculations (Table S1) predict that the strongest $WH_6(H_2)$ complex absorption will red shift 10−15 cm^{-1} from isolated WH_6, and the above 1925.7, 1911.5 and associated 515.6 cm^{-1} bands are best reassigned to $WH_6(H_2)$. At this point it is speculative, but the 1895.3 cm^{-1} band increases and decreases along with WH_4 on annealing and irradiation, and it could be due to a higher complex such as $WH_6(H_2)_2$ on the way to the final $WH_4(H_2)_4$ product.

Reaction Mechanism. The codeposition of W with pure HD contributes to our understanding of the reaction mechanism. The absence of bands for H−D and W−HD stretching modes in the 2200 and 1500 cm^{-1} regions along with the presence of major bands in the W−(H_2) and W−(D_2) stretching regions demonstrates that $WH_2D_2(HD)_x$ complexes are not formed. Furthermore, the intensities of bands in the W−H stretching region are substantially stronger than those in the W−D stretching region, in excess of the 2/1 relative intensity expected for H and D vibrational infrared intensities. Clear shifts occur in the strong W−H stretch to 1838.5 cm^{-1} and the W−D stretch to 1338.7 cm^{-1} relative to the all-H and all-D species, which shows that the WH_2D_2 primary hydride is formed (see calculated frequencies in Tables S2−S5). Thus, the spectrum in pure HD is dominated by the $WH_2D_2(H_2)_2(D_2)_2$ molecule. This suggests the participation of WH_6 in the mechanism of formation for $WH_4(H_2)_4$, which requires the dissociation of the reagent molecules and allows scrambling of the H and D in the products initially formed. The preference for WH_3D_3(short D) over WH_3D_3(long D) isotopic modifications and the fluxional nature of WH_6 owing to low barrier heights among the several structures have been noted.[11,12] Analogous isotopic scrambling has been observed in the Rh and Cr deuterium hydride systems.[26,27]

When the activated complexes produced in the exothermic reactions do finally relax, thermodynamic control leads to the formation of $WH_2D_2(H_2)_2(D_2)_2$ as opposed to $WH_2D_2(HD)_4$. The stability of one complex over the other cannot be assessed with regular computational methods, because we are in regime with the Born−Oppheneimer approximation. However, just looking at the computed zero-point energies, the $WH_2D_2(H_2)_2(D_2)_2$ isotopic molecule is the most stable species by 0.1 kcal/mol,

(25) (a) Scott, A. P.; Radom, L. *J. Phys. Chem.* **1996**, *100*, 16502. (b) Andersson, M. P.; Uvdal, P. L. *J. Phys. Chem. A* **2005**, *109*, 2937.

(26) Wang, X.; Andrews, L. *J. Phys. Chem. A* **2002**, *106*, 3706 (Rh + H_2).
(27) Wang, X.; Andrews, L. *J. Phys. Chem. A* **2003**, *107*, 570 (Cr + H_2).

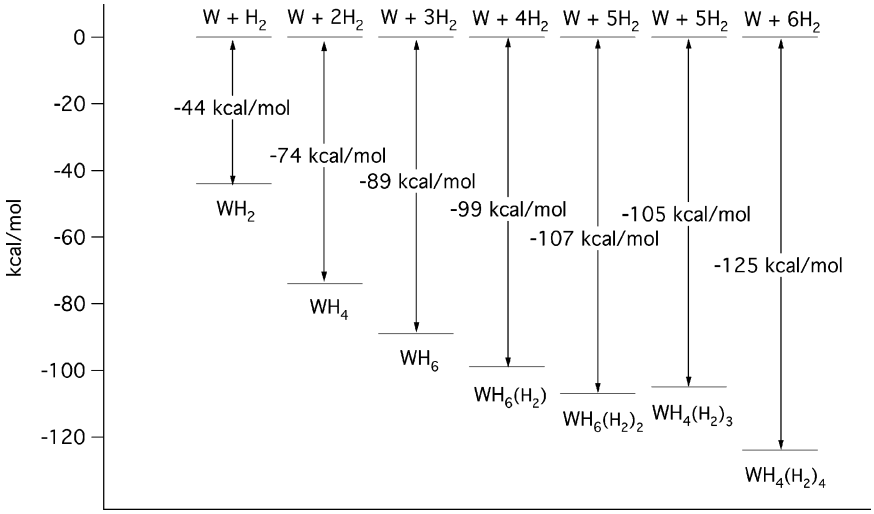

Figure 5. Energy level diagram for tungsten hydrides and dihydrogen complexes calculated at the BP86/TZVPP level of theory including zero-point energy correction but not basis set superposition error.

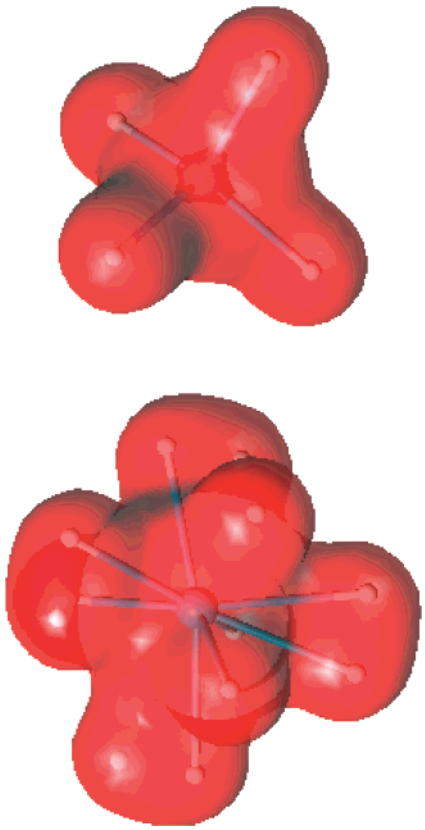

Figure 6. Electron density plots (0.04 iso density level) for WH_4 and the $WH_4(H_2)_4$ complex calculated at the CASSCF level of theory.

which is consistent with the above spectroscopic identification of this more stable isotopomer. This represents an isotopic exchange as the HD reagent allows the formation of WH_3D_3 in the structural form where the three D occupy the short bond positions owing to lower zero-point energy, which demonstrates the fluxional nature of WH_6.[12] Now the present pure HD experiment shows the formation of $WH_2D_2(H_2)_2(D_2)_2$ and not $WH_2D_2(HD)_4$ again owing to lower zero-point energy for the former complex. This also requires that the WH_4D_4 and WH_5D_5 complexes initially formed are sufficiently energized by reaction exothermicity to again equilibrate all of the H and D present. Then when the final WH_6D_6 species is formed, reaction energy activates randomization of H and D, and relaxation gives the most stable, based on zero-point energy, final $WH_2D_2(H_2)_2(D_2)_2$ complex, as observed in Figure 4a.

Bonding. Note that annealing in the neon matrix (Figure 1b, ref 7) increased WH_4, WH_6, and the bands we have reassigned here to the final $WH_4(H_2)_4$ product. This underscores the spontaneous reaction of tungsten atoms with hydrogen molecules to form this highest tetrahydride, tetradihydrogen complex. Figure 5 compares the reaction exothermicities for W atom reactions with *n* molecules of hydrogen to form the most stable hydrides and hydride complexes calculated at the BP86/TZVPP level of theory with zero-point energy correction. These energies are slightly higher using CCSD(T), CASPT2, and MP2, which in part accounts for dispersion interactions. The most significant point here is that four H_2 molecules are bound to WH_4 to form the physically stable $WH_4(H_2)_4$ tungsten hydride dihydrogen complex. Correction for BSSE further reduces these total binding energies to 50, 59, and 65 kcal/mol at the BP86, CASPT2, and MP2 levels of theory, respectively, for the four dihydrogen molecules. Since the MP2 approach is known to overestimate the interactions between closed shell fragments, more accurate calculations of the binding energy were performed at the CASPT2 and CCSD(T) levels of theory, using the DFT optimized structures. At the CCSD(T) level of theory, including the ZPE and BSSE corrections, the binding energy is predicted to be 56 kcal/mol. These highly correlated methods, CASPT2 and CCSD(T), thus predict a larger binding energy than DFT.

It is very interesting to consider the bonding of the H_2 molecules in the supercomplex species. There is definitely an electronic effect: in the triplet ground state of the WH_4 molecule the two unpaired electrons reside in two W 5d orbitals, while in the singlet ground state of the supercomplex the two electrons are paired and they reside in bonding orbitals between W and the H_2 moieties. It thus seems that the presence of the extra H_2 moieties has an electronic effect on WH_4, in the sense that it implies a bond formation between W and the H_2 moieties and a change in the ground state. The partial charges, according to a Mulliken analysis, are also different in the two cases. In WH_4, the W has a partial charge of $+1.57$, and the H, of -0.39, while, in $WH_4(H_2)_4$, the W has a partial charge of $+0.46$ and H(WH_4) has a partial charge of -0.18. The absolute values are probably

not relevant, but the relative values are interesting and they show that WH_4 becomes less ionic in the presence of the $4H_2$ moieties. Inspection of the total electron density calculated with a contour value of 0.03 for the two species indicates that a real bond occurs between the H_2 moieties and W (Figure 6). This is also confirmed by the values of the relevant bond distances computed at the DFT level of theory (Table 2): in WH_4 the W−H bond distance is 1.71 Å; in $WH_4(H_2)_4$ the W−H(hydride) bond distance is 1.74 Å, the W−H(H_2) bond distance is 1.85 Å and the H−H(H_2) bond distance is 0.88 Å. A similar calculation on an isolated H_2 molecule predicts a bond distance of 0.75 Å. As mentioned before, the MP2 results show a shorter W−H(H_2) bond length.

Conclusions

Laser-ablated W atoms codeposited with pure hydrogen at 4 K form a major product, which is identified as the $WH_4(H_2)_4$ complex on the basis of seven diagnostic infrared absorptions, their isotopic shifts, and agreement with isotopic frequencies calculated by density functional theory. This D_{2d} structured complex is calculated to form spontaneously from W atoms and hydrogen molecules. Warming the sample above 7 K allows the hydrogen matrix to evaporate and the complex to aggregate and ultimately to react with itself and decompose. Comparison of the H−H stretching mode at 2500 cm^{-1} and the W−H_2 stretching mode at 1782 cm^{-1} with 2690 and 1570 cm^{-1} values reported for the $W(CO)_3(PR_3)_2(H_2)$ complex[1a] suggests that the present physically stable $WH_4(H_2)_4$ complex has more strongly bound dihydrogen ligands. The average binding energy per dihydrogen ligand in our supercomplex is 15 kcal/mol computed at the CASPT2 level of theory. Hence, the four H_2 ligands interact strongly with WH_4 and alter the electronic state from triplet to singlet.

Acknowledgment. We gratefully acknowledge support for this research from the U.S. National Science Foundation under Grant No. CHE03-52487 and the Swiss National Science Foundation (Grant No. 200021-111645/1).

Supporting Information Available: Tables of calculated frequencies. This material is available free of charge via the Internet at http://pubs.acs.org.

JA077322O